Adaptive Sliding-Mode Control of an Offshore Container Crane With Unknown Disturbances

Gyoung-Hahn Kim, *Student Member, IEEE*, and Keum-Shik Hong, *Fellow, IEEE*

***Abstract*—In this paper, an adaptive sliding-mode control (ASMC) for offshore container cranes that load/unload containers from a mega container ship to a smaller vessel is investigated. To withstand the harsh working conditions in the open sea, such as ship motions and winds, a 4-degrees-of-freedom control model consisting of plant uncertainties and known/unknown disturbances is newly developed. After decoupling the actuated (i.e., trolley displacements) and unactuated (i.e., swing angles) joint variables, a sliding surface that incorporates the decoupled dynamics is designed. Then, a new sliding-mode control (SMC) algorithm with two adaptation laws for switching- and equivalent-control inputs is developed. The asymptotic stability to the "real" sliding surface introduced in the decoupled (actuated, unactuated) state space is proven without *a priori* knowledge on the bounds of unknown disturbances. For the experiment, a three-dimensional crane mounted on a Steward platform to generate the ship motions is utilized. To verify the effectiveness of the proposed ASMC method, experimental results of the proposed method are compared with two representative works: the SMC presented by Ngo and Hong and the ASMC presented by Zhu and Khayati. The vibration suppression capability of the proposed method in the presence of ship motions, large initial swings, parameter uncertainties, and sudden disturbances is superior to the two compared methods. The developed algorithm can be used for a mobile harbor system as a new tool in the modern maritime industry.**

***Index Terms*—Adaptive sliding-mode control (ASMC), mobile harbor, offshore container crane, underactuated mechanical system, vibration control.**

I. Introduction

OFFSHORE cranes, which are an important and indispensable means in modern maritime logistics, have been used to transfer loads in an open sea and for the maintenance of offshore installations. In recent years, there has been a substantial interest in offshore crane technologies after the "mobile harbor" (i.e., a vessel capable of container handling, mooring, and self-balancing) appeared as an alternative method to improve the handling efficiency of containers, which is limited by space in the conventional terminal, and avoid the unnecessary maritime latency of large container ships at a port [1], [2]. To achieve more efficient container handling tasks, a mobile harbor is mainly utilized to load/unload containers from a mega-size container ship in an open sea and move them to a nearby port or another container ship. This technology becomes feasible and consequently will realize high productivity in the intercontinental maritime logistics. In particular, a mobile harbor is highly expected to maximize its benefits in shallow water ports.

However, apart from the promising prospects, the practical operation of offshore container cranes remains challenging because of the harsh working conditions in the open sea. Disturbances, such as wave-induced ship motions (known disturbance) and wind gusts (unknown disturbance), persistently interfere with a fast and accurate crane operation. Thus, an advanced control technique that assures satisfactory performance is required to make the offshore container cranes usable for practical purposes. In this study, three control issues (modeling uncertainty, disturbance rejection, and robustness) are addressed to provide a solution for the effective and efficient operation of offshore container cranes under severe working conditions. An adaptive sliding-mode control (ASMC) strategy subjected to the roll and pitch motions of the mobile harbor and unknown disturbances is developed.

Over the past decades, extensive efforts have been made to control inland cranes (i.e., quay cranes, boom cranes, and tower cranes). Specifically, various closed-loop control methods have been employed, such as nonlinear quasi-PID control [3], delayed feedback control [4], feedback linearization control [5], [6], adaptive control [7], sliding mode control (SMC) [8]–[10], and nonlinear coupling control [11] to guarantee the robustness against the parameter uncertainties (load weight, friction, etc.) and disturbances. As an alternative method to the closed-loop control, open-loop control methods, including the time optimal control [12] and input shaping (or command shaping) control [13], [14], were often implemented to satisfy various demands from the industry (e.g., low cost and user convenience). However, the conventional methods developed for inland cranes cannot be applied to offshore container cranes because there are relative motions between two vessels (mobile harbor and mother ship, see Fig. 1), sea waves, and wind gusts. Thus, the ocean environment necessitates the development of a new control model and a new control technique that incorporates all of these issues.

Manuscript received March 30, 2019; revised August 10, 2019; accepted September 30, 2019. Date of publication October 7, 2019; date of current version December 31, 2019. This work was supported by the National Research Foundation of Korea under the Ministry of Science, ICT and Future Planning, Korea, under Grant NRF-2017R1A2A1A17069430. Recommended by Technical Editor Q. Xu. *(Corresponding author: Keum-Shik Hong.)*

The authors are with the School of Mechanical Engineering, Pusan National University, Busan 46241, South Korea (e-mail: hahn@pusan.ac.kr; kshong@pusan.ac.kr).

Color versions of one or more of the figures in this article are available online at http://ieeexplore.ieee.org.

Digital Object Identifier 10.1109/TMECH.2019.2946083

1083-4435 © 2019 IEEE. Personal use is permitted, but republication/redistribution requires IEEE permission.
See http://www.ieee.org/publications_standards/publications/rights/index.html for more information.

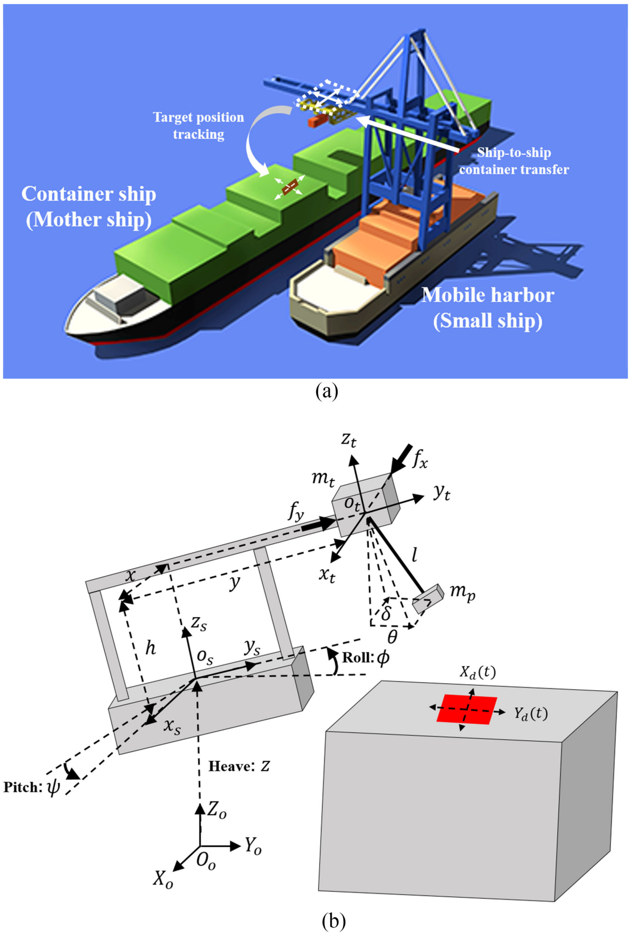

Fig. 1. Schematic of an offshore container crane working in the open sea. (a) Concept of a mobile harbor. (b) Defined coordinate frames.

Cranes (both inland and offshore) are underactuated mechanical systems, where there are fewer actuators than degrees of freedom. A main difference between inland and offshore container cranes is in the lateral dynamics of the payload. In the case of inland container cranes, the longitudinal sway motion of the payload is significant, and the lateral sway motion is negligible. However, in the case of offshore container cranes, the lateral sway angle of the payload caused by the pitch motion of the ship cannot be ignored. Therefore, two control inputs (traveling and traversing motions of the trolley) in the case of offshore container cranes are required to suppress both longitudinal and lateral sway angles simultaneously. The control strategies for the underactuated inland systems are diverse, which include a normal form transformation approach [15], decoupling procedure [16], SMC [17]–[19], terminal SMC [20]–[22], robust adaptive control [23]–[26], state-constrained adaptive fuzzy control [27]–[29], energy-based control [30], boundary control [31], etc. However, the control of an offshore underactuated system is not straightforward. In this paper, after a systematic decoupling of actuated/unactuated dynamics for offshore systems, an ASMC law to simultaneously suppress both longitudinal and lateral sway angles with two trolley inputs is developed.

In contrast to numerous studies on inland cranes, the results on ship-mounted cranes are rare. For a floating crane, the equations of motion and the associated nonlinear dynamical behavior analysis including bifurcation were investigated in [32], [33]. For ship-mounted boom cranes, several methods were proposed: a delayed-position feedback control to suppress the sway of the payload by manipulating the slew and luff angles of the boom [34], LQG and generalized predictive control using a linear model [35], a rate-based control strategy (i.e., using the velocities of the ship) to stabilize the payload [36], a PID control with an auxiliary system for a simplified offshore jib crane model [37], various energy-based control laws based on Lyapunov functions [38]–[41], and an adaptive repetitive learning control for a boom crane [42].

However, related to the offshore container cranes between two ships, only a few studies were reported. Since the relative motions of the ships/cranes are involved and the external disturbances are large, Hong and Ngo [1] investigated for the first time a mathematical model for a mobile harbor in the presence of the sea-excited ship motions, and they proposed an SMC method in [2]. Tuan *et al.* discussed a feedback linearization control [43] and a backstepping SMC [44] assuming an "ideal" model that the roll and pitch motions of the ship could be generated by a mass–spring–damper system. Ismail *et al.* [45] designed an optimal SMC for a linear offshore container crane model. Kim and Park [46] presented a preview tracking control using a linearized model and a parameter identification technique based on the experimental results from a scaled-down offshore container crane. Recently, Ngo *et al.* [47] presented a fuzzy SMC with the Kalman filter to solve a control problem of the system with measurement noise.

Despite the continuous efforts in the past, many problems, such as safety and efficiency, remain unsolved. For example, most existing closed-loop control methods were developed using a 3-degrees-of-freedom (3-DOF) model (i.e., longitudinal trolley motion and the longitudinal and lateral sway angles of the payload) to position the payload to a stationary target location. However, in practice, the control performance of such methods will be degraded in the ocean: The roll and pitch motions of a container ship make the target position of the payload vary in time, which requires both longitudinal and lateral movements of the trolley. In addition, by assuming small sway angles of the payload and small roll and pitch motions of the ships, a linear model and subsequently linear control laws were developed [45], [46]. The robustness of the developed control algorithm was not answered in [1], [2], [43]–[47], which degraded the performance in the presence of unknown disturbances or even instability under a severe working condition.

In this paper, an ASMC is proposed based on a nonlinear 4-DOF model for offshore container cranes with unknown disturbances. The contributions of the paper are summarized as follows.

1) A 4-DOF nonlinear model for offshore container cranes is established for the first time by considering the longitudinal/lateral trolley dynamics and unknown matched/unmatched disturbances.

2) A systematic decoupling scheme between trolley dynamics and sway dynamics is presented in designing a sliding surface between the unactuated state variables (sway angles) and the actuated state variables (trolley displacements).
3) Based on the obtained model and proposed decoupling scheme, a new ASMC algorithm is developed by proposing two adaptation laws, which can overcome the performance degradation resulting from the chattering and inaccurate equivalent control.
4) The proposed control law ensures the asymptotic stability of the sliding surface even in the presence of parametric uncertainties (cargo weight, rope length) and matched and unmatched unknown disturbances. Furthermore, the stability proof does not require *a priori* known bounds on the disturbances.
5) With a three-dimensional (3-D) crane mounted on a 6-DOF motion simulator (a Stewart platform), the effectiveness of the proposed method in comparison with the two existing methods is validated. The tracking performance of the proposed method in the presence of the ship roll and pitch motions and the wind-induced sudden impact is demonstrated in experiments while transporting a load to its time-varying target locations.

The paper is organized as follows. In Section II, the dynamics of an offshore container crane is described, and a model decoupling method is developed to separate the dynamics into two subsystems: actuated and unactuated dynamics. In Section III, a novel ASMC is developed for the 4-DOF offshore container crane, and its stability is proven using the Lyapunov theory. In Section IV, experimental results are provided to illustrate the performance of the proposed control scheme. The main findings are summarized in Section V.

II. Problem Statement

The offshore container crane considered in this paper is a type of cranes that operate on top of a mobile harbor [1], where a dual-stage trolley (i.e., the main longitudinal traveling mechanism and an auxiliary lateral traversing mechanism) is utilized to load and unload containers to and from their time-varying target positions on the container ship. Fig. 1(a) illustrates a schematic of the container transportation with the offshore container crane. Fig. 1(b) shows the introduced coordinate systems to derive the equations of motion of the payload (i.e., container). Let $\{X_o, Y_o, Z_o\}$ denote the reference coordinate frame, and $\{x_s, y_s, z_s\}$ indicates the ship coordinate frame with the origin o_s at the center of gravity of the ship. Assuming that under a balancing mechanism of the ship, the crane coordinate frame coincides with the ship coordinate frame. Let $\{x_t, y_t, z_t\}$ be the trolley coordinate frame affixed to the trolley; m_p, m_t, l, and h are the payload mass, trolley mass, rope length, and crane height, respectively. Let δ and θ describe the rotational angles of the payload along the X_o- and Y_o-axis in the reference coordinate frame. Now, in the crane coordinate frame, x and y indicate the lateral and longitudinal displacements of the trolley, respectively, and f_x and f_y are the control forces applied at the trolley in the x and y directions, respectively, in the crane coordinate frame. As shown in Fig. 1(b), ϕ, ψ, and z describe the roll, pitch, and heave motions of the mobile harbor, respectively. Since the mobile harbor and mother ship are moored together by a special docking mechanism, the yaw, surge, and sway motions of the mobile harbor are assumed to be small in the ship coordinate frame. The following assumptions are made.

Assumption 1: The payload is supposed to be a point mass (i.e., the rotational motion of the payload is not considered in this paper), and the rope is a massless rigid rod (i.e., not a flexible link).

Assumption 2: Wave-induced ship motions are bounded: The roll, pitch, and heave motions of the mobile harbor and their first and second derivatives satisfy the following inequalities:

$$\begin{aligned} &|\phi| \le \mu_1, \left|\dot{\phi}\right| \le \mu_2, \left|\ddot{\phi}\right| \le \mu_3, \\ &|\psi| \le \mu_4, \left|\dot{\psi}\right| \le \mu_5, \left|\ddot{\psi}\right| \le \mu_6, \\ &|z| \le \mu_7, |\dot{z}| \le \mu_8, |\ddot{z}| \le \mu_9 \end{aligned} \tag{1}$$

where μ_i $(i = 1, \ldots 9)$ are positive constants.

A. Dynamics With the Matched and Unmatched Disturbances

Based on the coordinate systems in Fig. 1(b), trolley position p_t and payload position p_l in the reference coordinate frame are obtained as follows:

$$p_t = \begin{bmatrix} x \cos\psi + y \sin\psi\sin\phi + h\sin\psi\cos\phi \\ y\cos\phi - h\sin\phi \\ z - x\sin\psi + y\cos\psi\sin\phi + h\cos\psi\cos\phi \end{bmatrix}, \tag{2}$$

$$p_l = \begin{bmatrix} x\cos\psi + y\sin\psi\sin\phi + h\sin\psi\cos\phi - l\cos\theta\sin\delta \\ y\cos\phi - h\sin\phi + l\sin\theta \\ z - x\sin\psi + y\cos\psi\sin\phi + h\cos\psi\cos\phi - l\cos\theta\cos\delta \end{bmatrix}. \tag{3}$$

Then, using Lagrange's method, the equations of motion of the trolley and payload are obtained as follows:

$$M(q)\ddot{q} + C(q,\dot{q})\dot{q} + G(q) = u + f_d + \Delta \tag{4}$$

where

$$M(q) = \begin{bmatrix} m_{11} & 0 & m_{13} & m_{14} \\ 0 & m_{22} & m_{23} & m_{24} \\ m_{31} & m_{32} & m_{33} & 0 \\ m_{41} & m_{42} & 0 & m_{44} \end{bmatrix}, C(q,\dot{q}) = \begin{bmatrix} 0 & c_{12} & c_{13} & c_{14} \\ c_{21} & 0 & c_{23} & c_{24} \\ c_{31} & c_{32} & c_{33} & c_{34} \\ c_{41} & c_{42} & c_{43} & 0 \end{bmatrix},$$

$$G(q) = [g_1\ g_2\ g_3\ g_4]^T, u = [u_x\ u_y\ 0\ 0]^T,$$

$$f_d = [f_{d1}\ f_{d2}\ f_{d3}\ f_{d4}]^T, \Delta = [\Delta_x\ \Delta_y\ \Delta_\delta\ \Delta_\theta]^T$$

and the components of the matrices are

$$m_{11} = m_t + m_p, m_{13} = m_{31} = -m_p l\cos\theta\cos(\delta - \theta),$$

$$m_{14} = m_{41} = m_p l\sin\theta\sin(\delta - \psi),$$

$$m_{22} = m_t + m_p, m_{23} = m_{32} = m_p l \sin\phi \cos\theta \sin(\delta - \psi),$$
$$m_{24} = m_p l \sin\phi \sin\theta \cos(\delta - \psi) + m_p l \cos\phi \cos\theta,$$
$$m_{33} = m_p l^2 \cos^2\theta, m_{42} = m_{24}, m_{44} = m_p l^2,$$
$$c_{12} = (m_t + m_p)\dot{\psi} \sin\phi, c_{21} = -(m_t + m_p)\dot{\psi}\sin\phi,$$
$$c_{13} = m_p l\dot{\delta}\cos\theta \sin(\delta - \psi) + m_p l\dot{\theta}\sin\theta\cos(\delta - \psi),$$
$$c_{14} = m_p l\dot{\theta}\cos\theta \sin(\delta - \psi) + m_p l\dot{\delta}\sin\theta\cos(\delta - \psi),$$
$$c_{23} = m_p l\dot{\delta}\sin\phi\cos\theta\cos(\delta - \psi) - m_p l\dot{\theta}\sin\phi\sin\theta\sin(\delta - \psi),$$
$$c_{24} = m_p l\dot{\theta}\sin\phi\cos\theta\cos(\delta - \psi) - m_p l\dot{\theta}\cos\phi\sin\theta - m_p l\dot{\delta}\sin\phi\sin\theta\sin(\delta - \psi),$$
$$c_{31} = -m_p l\dot{\psi}\cos\theta\sin(\delta - \psi),$$
$$c_{32} = -m_p l\dot{\psi}\cos\theta\sin(\delta - \psi),$$
$$c_{32} = -m_p l\dot{\psi}\cos\theta\sin(\delta - \psi),$$
$$c_{32} = -m_p l\dot{\psi}\cos\theta\sin(\delta - \psi),$$
$$c_{32} = -m_p l\dot{\psi}\cos\theta\sin(\delta - \psi),$$
$$c_{32} = -m_p l\dot{\psi}\sin\phi\cos\theta\cos(\delta - \psi) + m_p l\dot{\phi}\cos\theta\cos\phi\sin(\delta - \psi),$$
$$c_{33} = -m_p l\dot{\psi}\cos\theta\sin(\delta - \psi),$$
$$c_{32} = -m_p l^2\dot{\theta}\sin\theta\cos\theta, c_{34} = -m_p l^2\dot{\delta}\sin\theta\cos\theta,$$
$$c_{41} = -m_p l\dot{\psi}\sin\theta\cos(\delta - \psi),$$
$$c_{42} = m_p l\dot{\psi}\sin\phi\sin\theta\sin(\delta - \psi) - m_p l\dot{\phi}\sin\phi\cos\theta + m_p l\dot{\phi}\cos\phi\sin\theta\cos(\delta - \psi),$$
$$c_{43} = m_p l^2\dot{\delta}\sin\theta\cos\theta,$$
$$g_1 = -(m_t + m_p)\dot{\psi}^2 x + (m_t + m_p)(\ddot{\psi}\sin\phi + 2\dot{\psi}\dot{\phi}\cos\phi)y - (m_t + m_p)(g + \ddot{z})\sin\psi,$$
$$g_2 = -(m_t + m_p)\ddot{\psi}x\sin\phi - (m_t + m_p)(\dot{\psi}^2\sin^2\phi + \dot{\phi}^2)y - (m_t + m_p)(g - \ddot{z})\cos\psi\sin\phi,$$
$$\begin{aligned} g_3 = &- m_p lh\ddot{\psi}\cos\theta\cos\phi\cos(\delta - \psi) \\ &- m_p lh\ddot{\phi}\cos\theta\sin\phi\sin(\delta - \psi) + m_p l(g + \ddot{z}) \sin\delta\cos\theta \\ &- m_p lh(\dot{\phi}^2 + \dot{\psi}^2)\cos\phi\cos\theta\sin(\delta - \psi) \\ &+ 2m_p lh\dot{\phi}\dot{\psi}\sin\phi\cos\theta\cos(\delta - \psi) \\ &- m_p lx\cos\theta(\ddot{\psi}\sin(\delta - \psi) - \dot{\psi}^2\cos(\delta - \psi)) \\ &+ m_p ly\cos\theta(\ddot{\phi}\cos\phi\sin(\delta - \psi) - \ddot{\psi}\sin\phi \cos(\delta - \psi)) \\ &- m_p ly\cos\theta(\dot{\phi}^2 + \dot{\psi}^2)\sin\phi\sin(\delta - \psi)) \\ &- 2m_p l\dot{\psi}\dot{\phi}y\cos\theta\cos\phi\cos(\delta - \psi), \end{aligned}$$
$$\begin{aligned} g_4 = &- 2m_p lh\dot{\phi}\dot{\psi}\sin\phi\sin\theta\sin(\delta - \psi) \\ &- m_p lh\ddot{\phi}(\sin\theta\sin\phi\cos(\delta - \psi) + \cos\phi\cos\theta) \\ &+ m_p l(g + \ddot{z})\sin\theta\cos\delta + m_p lh\dot{\phi}^2\sin\phi\cos\theta \\ &- m_p lh(\dot{\phi}^2 + \dot{\psi}^2)\cos\phi\cos\theta\sin(\delta - \psi) \\ &+ m_p lh\ddot{\psi}\cos\phi\sin\theta\sin(\delta - \psi) \\ &- m_p lx\sin\theta(\dot{\psi}^2\sin(\delta - \psi) + \ddot{\psi}\cos(\delta - \psi)) \\ &+ m_p ly\sin\theta(\ddot{\psi}\sin\phi\sin(\delta - \psi) + \ddot{\phi}\cos\phi \cos(\delta - \psi)) \\ &- m_p ly\cos\theta(\dot{\phi}^2\cos\phi + \ddot{\phi}\sin\phi) \\ &+ 2m_p l\dot{\psi}\dot{\phi}y\sin\theta\cos\phi\sin(\delta - \psi) \\ &- m_p ly\sin\phi\sin\theta\cos(\delta - \psi)(\dot{\phi}^2 + \dot{\psi}^2), \end{aligned}$$
$$f_{d1} = -h(m_t + m_p)(\ddot{\psi}\cos\phi - 2\dot{\psi}\dot{\phi}\sin\phi) - (m_t + m_p)\dot{y}\dot{\psi}\sin\phi,$$
$$f_{d2} = h(m_t + m_p)(\dot{\psi}^2\sin\phi\cos\phi + \ddot{\phi}) + (m_t + m_p)\dot{x}\dot{\psi}\sin\phi,$$
$$f_{d3} = m_p l\dot{y}\cos\theta(\dot{\psi}\sin\phi\cos(\delta - \psi) - \dot{\phi}\cos\phi\sin(\delta - \psi)) + m_p l\dot{x}\dot{\psi}\cos\theta\sin(\delta - \psi),$$
$$f_{d4} = -m_p l\dot{\psi}\dot{y}\sin\phi\sin\theta\sin(\delta - \psi) + m_p l\dot{x}\dot{\psi}\sin\theta \cos(\delta - \psi) + m_p l\dot{\phi}\dot{y}(\sin\phi\cos\theta - \cos\phi\sin\theta\cos(\delta - \psi)).$$

In (4), $q = [x\ y\ \delta\ \theta]^T$ is the state vector; $M(q) \in \mathbb{R}^{4\times 4}$ and $C(q, \dot{q}) \in \mathbb{R}^{4\times 4}$ represent the inertia and Coriolis–centripetal matrices, respectively; $G(q) \in \mathbb{R}^4$ denotes the gravity vector; $u \in \mathbb{R}^4$ is the control input vector. For disturbances, $f_d \in \mathbb{R}^4$ are the known disturbances related to the ship motions induced by waves and winds, whereas $\Delta \in \mathbb{R}^4$ are the unknown disturbances (either matched or unmatched) comprising modeling uncertainties and other negative effects, such as sea winds. Additionally, the dynamics in (4) satisfies the following properties on the inertia and Coriolis–centripetal matrices and the disturbance vectors.

Property 1 [38]: $M(q)$ is a positive-definite symmetrical bounded matrix, i.e., there are positive constants m_L and m_U such that $m_L\|\xi\|^2 \le \xi^T M(q)\xi \le m_U\|\xi\|^2$, where $\xi \in \mathbb{R}^4$.

Property 2 [38]: Matrix $\dot{M} - 2C$ is a skew-symmetric matrix, i.e., $\xi^T[\dot{M}(q)/2 - C(q, \dot{q})]\xi = 0$, where $\xi \in \mathbb{R}^4$.

Property 3 [42]: The known disturbance vector f_d satisfies $\|f_d\| < \bar{f}_d$, where $\bar{f}_d \in \mathbb{R}^+$ is an *a priori* known positive constant. The unknown disturbance vector Δ satisfies $\|\Delta\| < \bar{\Delta}^*$, where $\bar{\Delta}^* \in \mathbb{R}^+$ is an unknown positive constant.

Remark 1: Properties 1 and 2 hold for other dynamical systems derived by Lagrange's equation, including the inland cranes

[3]–[11]. Property 3 is a reasonable assumption from the sense that the structure of known disturbances is available, and the parameters in the structure are practically accessible, whereas the parameters of unknown disturbances are neither given nor measurable.

Remark 2: The persistent ship movements (ϕ, ψ) enter as time-varying terms in the inertia matrix $M(q)$, Coriolis- centripetal matrix $C(q, \dot{q})$, and gravity vector $G(q)$; they also become structured disturbances in the explicit form (i.e., f_d). In addition, other pure disturbances (i.e., Δ) are introduced in an unstructured form to represent the unknown disturbances. In particular, the unknown disturbances that act on the unactuated part in the crane dynamics (i.e., the unmatched disturbances in the δ and θ dynamics) are extremely difficult to handle theoretically. All previous works [1], [2], [43]–[47] were based on a problem formulation that only considered the structured disturbance f_d induced by the ship motions.

B. Model Decoupling

State vector q is now split into two parts: actuated joint variables $q_a \in \mathbb{R}^2$ (i.e., x and y) and unactuated joint variables $q_u \in \mathbb{R}^2$ (i.e., δ and θ), where the subscripts a and u denote the actuated and unactuated variables, respectively. The equations of motion (4) are rewritten as follows:

$$M_{11}(q)\ddot{q}_a + M_{12}(q)\ddot{q}_u + N_a(q,\dot{q}) = u_a + \Delta_a, \tag{5a}$$

$$M_{21}(q)\ddot{q}_a + M_{22}(q)\ddot{q}_u + N_u(q,\dot{q}) = \Delta_u \tag{5b}$$

where

$$M_{11}(q) = \begin{bmatrix} m_{11} & 0 \\ 0 & m_{22} \end{bmatrix}, M_{12}(q) = \begin{bmatrix} m_{13} & m_{14} \\ m_{23} & m_{24} \end{bmatrix},$$

$$M_{21}(q) = \begin{bmatrix} m_{31} & m_{32} \\ m_{41} & m_{42} \end{bmatrix}, M_{22}(q) = \begin{bmatrix} m_{33} & 0 \\ 0 & m_{44} \end{bmatrix},$$

$$N_a(q,\dot{q}) = C_{11}(q,\dot{q})\dot{q}_a + C_{12}(q,\dot{q})\dot{q}_u + G_a(q) - f_{da},$$

$$N_u(q,\dot{q}) = C_{21}(q,\dot{q})\dot{q}_a + C_{22}(q,\dot{q})\dot{q}_u + G_u(q) - f_{du},$$

$$\Delta_a = [\Delta_x \quad \Delta_y]^T, \Delta_u = [\Delta_\delta \quad \Delta_\theta]^T, u_a = [u_x \quad u_y]^T$$

and

$$C_{11}(q,\dot{q}) = \begin{bmatrix} 0 & c_{12} \\ c_{21} & 0 \end{bmatrix}, C_{12}(q,\dot{q}) = \begin{bmatrix} c_{13} & c_{14} \\ c_{23} & c_{24} \end{bmatrix},$$

$$C_{21}(q,\dot{q}) = \begin{bmatrix} c_{31} & c_{32} \\ c_{41} & c_{42} \end{bmatrix}, C_{22}(q,\dot{q}) = \begin{bmatrix} c_{33} & c_{34} \\ c_{43} & 0 \end{bmatrix},$$

$$G_a(q) = [g_1 \quad g_2]^T, G_u(q) = [g_3 \quad g_4]^T,$$

$$f_{da} = [f_{d1} \quad f_{d2}]^T, f_{du} = [f_{d3} \quad f_{d4}]^T.$$

Considering that M_{22} is a symmetric positive definite matrix for every $q \in \mathbb{R}^4$, (5b) becomes

$$\ddot{q}_u = -M_{22}^{-1}(M_{21}\ddot{q}_a + N_u - \Delta_u). \tag{6}$$

Substituting (6) into (5a), (5a) becomes

$$M_{11}\ddot{q}_a - M_{12}M_{22}^{-1}(M_{21}\ddot{q}_a + N_u - \Delta_u) + N_a = u_a + \Delta_a. \tag{7}$$

Rearranging terms in (7), it becomes

$$\ddot{q}_a = \bar{M}_{11}(u_a + \Delta_a - N_a) + \bar{M}_{12}(\Delta_u - N_u) \tag{8}$$

where

$$\bar{M}_{11} = (M_{11} - M_{12}M_{22}^{-1}M_{21})^{-1},$$

$$\bar{M}_{12} = -(M_{11} - M_{12}M_{22}^{-1}M_{21})^{-1}M_{12}M_{22}^{-1}.$$

Next, the substitution of (8) into (6) yields

$$\ddot{q}_u = \bar{M}_{21}(u_a + \Delta_a - N_a) + \bar{M}_{22}(\Delta_u - N_u) \tag{9}$$

where

$$\bar{M}_{21} = \bar{M}_{12}^T = -(M_{22} - M_{21}M_{11}^{-1}M_{12})^{-1}M_{21}M_{11}^{-1},$$

$$\bar{M}_{22} = (M_{22} - M_{21}M_{11}^{-1}M_{12})^{-1}.$$

Then, (5a) and (5b) can be expressed in the decoupled form as follows:

$$\ddot{q}_a = \eta_a(q,\dot{q}) + b_a(q)[d_{ma} + u_a] + d_{ua}, \tag{10a}$$

$$\ddot{q}_u = \eta_u(q,\dot{q}) + b_u(q)[d_{mu} + u_a] + d_{uu} \tag{10b}$$

where

$$\eta_a(q,\dot{q}) = -\bar{M}_{11}N_a - \bar{M}_{12}N_u, b_a(q) = \bar{M}_{11},$$

$$\eta_u(q,\dot{q}) = -\bar{M}_{21}N_a - \bar{M}_{22}N_u, b_u(q) = \bar{M}_{21},$$

$$d_{ma} = d_{mu} = \Delta_a, d_{ua} = \bar{M}_{12}\Delta_u, d_{uu} = \bar{M}_{22}\Delta_u.$$

III. Controller Design

A. Control Objective

The control objective in this paper is to achieve the tracking performance of the dual-stage trolley for a desired target position $(x_d(t), y_d(t))$ while making the cargo swing angles zero $(\delta_d = 0, \theta_d = 0)$ at the goal position. Let $e = [e_x, e_y, e_\delta, e_\theta]^T = [x - x_d, y - y_d, \delta, \theta]^T$ be the error vector. Then, the error dynamics are obtained as follows:

$$\ddot{e}_a = \eta_a(e,\dot{e}) + b_a(e)[d_{ma} + u_a] + d_{ua},$$

$$\ddot{e}_u = \eta_u(e,\dot{e}) + b_u(e)[d_{mu} + u_a] + d_{uu}. \tag{11}$$

Now, the convergence of error vector $\boldsymbol{e}$ to zero must be ensured.

B. Trajectory Planning

In contrast to inland cranes where the target position is stationary, the offshore container cranes must transfer containers in the presence of relative motions between the mother ship and a smaller vessel. Therefore, the desired reference signal varies in time. In practice, the target position $(X_d(t), Y_d(t))$ is given with respect to the reference coordinate frame. Thus, their corresponding values in the crane coordinate frame must be computed by coordinate transformations. In this paper, using (2), the desired trajectories $(x_d(t), y_d(t))$ in the crane coordinate frame are given as follows:

$$x_d(t) = [X_d(t) - Y_d(t)\sin\psi\sin\phi - h\sin\psi\cos\phi]/\cos\psi,$$

$$y_d(t) = [Y_d(t) + h\sin\phi]/\cos\phi \tag{12}$$

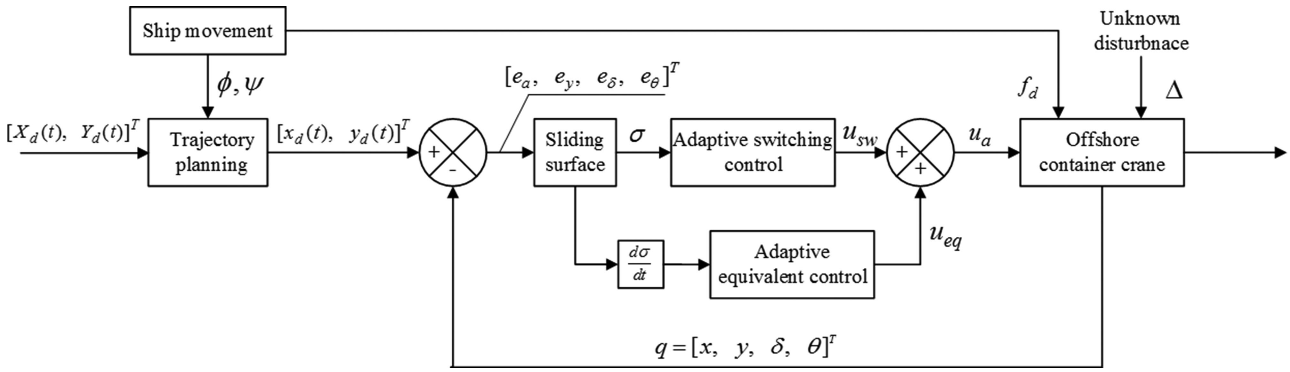

Fig. 2. Block diagram of the proposed ASMC.

where the time-varying target position $(X_d(t), Y_d(t))$ caused by the roll and pitch motions of the container ship is assumed to exhibit an *X*–*Y* planar trajectory. In this paper, the rotational motions of the load are not considered, which require additional skew, list, and trim controls by adjusting the lengths of individual hoisting ropes.

C. Adaptive Sliding-Mode Control

Fig. 2 shows a block diagram of the proposed ASMC method. To find a feedback control input u such that output q tracks the desired trajectory q_d and tracking error e asymptotically converges to zero, a sliding surface $\sigma = [\sigma_1, \sigma_2]^T$ is designed as follows:

$$\sigma = \dot{e}_a + \lambda_1 e_a + \lambda_2 \dot{e}_u + \lambda_3 e_u \tag{13}$$

where $\lambda_1 = \begin{bmatrix} \lambda_{11} & 0 \\ 0 & \lambda_{12} \end{bmatrix}$, $\lambda_2 = \begin{bmatrix} \lambda_{21} & 0 \\ 0 & \lambda_{22} \end{bmatrix}$, and $\lambda_3 = \begin{bmatrix} \lambda_{31} & 0 \\ 0 & \lambda_{32} \end{bmatrix}$ are diagonal matrices, whose design parameters satisfy the following sufficient conditions:

$$\lambda_{11}, \lambda_{12} > 0, \lambda_{31}/\lambda_{21}, \lambda_{32}/\lambda_{22} > 0. \tag{14}$$

In particular, λ_{21} and λ_{22} are nonzero but very small constants, that is

$$|\lambda_{21}|, |\lambda_{22}| \cong 0. \tag{15}$$

Next, by taking the time derivative of (13), the σ-dynamics becomes the following:

$$\dot{\sigma} = \Psi + \tilde{\Psi} + \Gamma u_a = \bar{\Psi} + \Gamma u_a \tag{16}$$

where $\Psi = \eta_a + \lambda_1 \dot{e}_a + \lambda_2 \eta_u + \lambda_3 \dot{e}_u$, $\tilde{\Psi} = b_a d_{ma} + d_{ua} + \lambda_2 b_u d_{mu} + \lambda_2 d_{uu}$, and $\Gamma = b_a + \lambda_2 b_u$. Then, based on the sliding surface (13) and sliding dynamics (16), the proposed ASMC law is obtained as follows:

$$u_a = \begin{cases} u_{\mathrm{eq}} - K(t)\frac{\sigma}{\|\sigma\|} & \text{if } \sigma \neq 0 \\ u_{\mathrm{eq}} & \text{if } \sigma = 0 \end{cases} \tag{17}$$

where the first term $u_{\mathrm{eq}} \in \mathbb{R}^2$ is the equivalent control to be later designed, and the second term is the adaptive switching control (or discontinuous scaled unit-vector control), where the adaptation law for the disturbance compensation and minimum chattering is defined as follows:

$$\begin{cases} \dot{K}^* = \alpha\,\|\sigma\| \cdot \mathrm{sgn}(\|\sigma\| - \varepsilon) \\ K = K^* + \beta(e^{\|\sigma\|} - 1). \end{cases} \tag{18}$$

Here $\alpha > 0$ and $\beta > 0$ are the design parameters in association with the convergence speed, and $\varepsilon > 0$ is a tunable positive small constant with respect to the real sliding mode defined as follows.

Definition 1 [48]: Let $\Sigma = \{x \in \chi = [e_a^T, \dot{e}_a^T, e_u^T, \dot{e}_u^T]^T \subset \mathbb{R}^8 | \|\sigma(x,t)\| \leq \varepsilon\}$ be locally an integral set in the Filippov sense. The corresponding behavior of system (11) on Σ is called the "real sliding mode" with respect to the sliding vector σ.

This concept concerning the real sliding mode is related to the practical implementation of the ASMC and stability proof. To complete the derivation of control law (17), the equivalent control u_{eq} is determined without uncertainties ($\tilde{\Psi} = 0$) using

$$\dot{\sigma} = 0. \tag{19}$$

In other words, the equivalent control is obtained by solving (19) for variable u_{eq} given by

$$u_{\mathrm{eq}} = -\Gamma^{-1}\Psi. \tag{20}$$

Remark 3: Basically, the equivalent control input (20) is used to directly eliminate the nonlinear dynamics, so that all state trajectories depart from the sliding manifold when the real sliding mode occurs. However, in practical applications, such equivalent control input based on an inaccurate mathematical model can limit the control performance due to adverse effects, such as the chattering phenomena despite the adaptive algorithm in (18). Specifically, the ASMC method presented in [49]–[51] reported that such unexpected performance degradation was observed in experiments.

In this paper, to avoid the aforementioned performance degradation, a new adaptive algorithm is introduced in the equivalent control law. Let $\hat{\Psi} = [\hat{\Psi}_1, \hat{\Psi}_2]^T$ be the estimated vector of Ψ and $[e_{\Psi_1}, e_{\Psi_2}]^T = [\Psi_1 - \hat{\Psi}_1, \Psi_2 - \hat{\Psi}_2]^T$ be the estimation errors. Now, the adaptive laws for Ψ are proposed as follows:

$$\begin{aligned} \dot{e}_{\Psi_1} &= -2\kappa_1(\dot{e}_x + \lambda_{11}e_x + \lambda_{21}\dot{e}_\delta + \lambda_{31}e_\delta), \\ \dot{e}_{\Psi_2} &= -2\kappa_2(\dot{e}_y + \lambda_{12}e_y + \lambda_{22}\dot{e}_\theta + \lambda_{32}e_\theta) \end{aligned} \tag{21}$$

where parameters κ_1 and κ_2 are positive constants, which indicate the adaptive gains. Then, instead of (20), a new adaptive equivalent control law using the estimated Ψ is proposed as follows:

$$u_{\mathrm{eq}} = -\Gamma^{-1}\hat{\Psi}. \tag{22}$$

Now, the following lemma is introduced to analyze the stability of the proposed feedback control system.

Lemma 1 [49]: Matrix $\Gamma \in \mathbb{R}^{2\times 2}$ is positive definite in a wider sense, i.e., its symmetric part Γ_s, which is defined by

$$\Gamma_s = (\Gamma + \Gamma^T)/2 \tag{23}$$

is positive definite in the regular meaning. Particularly, if $m = 1$, the scalar term Γ has a lower bound as follows:

$$0 \le \underline{\Gamma} \le \Gamma. \tag{24}$$

Proof: To prove Lemma 1, Γ and its transpose Γ^T are inserted into (23), and $(\Gamma + \Gamma^T)/2$ is evaluated. Since the computation is straightforward, the remainder is omitted for brevity by noting that $\Gamma_s\ (1,\, 1) > 0$ (i.e., the first element of Γ_s is positive) and $det\,(\Gamma_s) > 0$.

Theorem 1: Consider an offshore container crane system in (11) with the sliding dynamics of (16). Then, the control law (17) with the adaptive switching gain (18) and the adaptive equivalent control u_{eq} defined in (22) assures that for any initial condition $\|\sigma\| > \varepsilon$, the sliding variable σ converges to the domain $\|\sigma\| \le \varepsilon$ within a finite time $t_f > 0$ and remains in the domain for all $t \ge t_f$.

Proof: Let us choose a nonnegative Lyapunov function in the following form:

$$V = \sigma^T\sigma + \frac{1}{2\kappa_1}e^2_{\Psi_1} + \frac{1}{2\kappa_2}e^2_{\Psi_2}. \tag{25}$$

Differentiating both sides of V with respect to time yields

$$\begin{aligned}\dot{V} &= \dot{\sigma}^T\sigma + \sigma^T\dot{\sigma} + \frac{1}{\kappa_1}e_{\Psi_1}\dot{e}_{\Psi_1} + \frac{1}{\kappa_2}e_{\Psi_2}\dot{e}_{\Psi_2}\\ &= 2\sigma^T\tilde{\Psi} - \frac{K}{\|\sigma\|}\left(\sigma^T\Gamma^T\sigma + \sigma^T\Gamma\sigma\right).\end{aligned} \tag{26}$$

Using Lemma 1, the following equation is obtained:

$$\begin{aligned}\dot{V} &= 2\left[\sigma^T\tilde{\Psi} - \frac{K}{\|\sigma\|}\left(\sigma^T\Gamma_s\sigma\right)\right] = 2\,\|\sigma\|\left[\frac{\sigma^T\tilde{\Psi}}{\|\sigma\|} - K\frac{\sigma^T\Gamma_s\sigma}{\sigma^T\sigma}\right]\\ &= 2\,\|\sigma\|\left[\frac{\sigma^T\tilde{\Psi}}{\|\sigma\|} - \beta\left(e^{\|\sigma\|}-1\right)\frac{\sigma^T\Gamma_s\sigma}{\sigma^T\sigma} - K^*\frac{\sigma^T\Gamma_s\sigma}{\sigma^T\sigma}\right]\\ &= 2\,\|\sigma\|\left[\Omega(t) - K^*\frac{\sigma^T\Gamma_s\sigma}{\sigma^T\sigma}\right].\end{aligned} \tag{27}$$

Here, scalar $\Omega(t)$ has an upper bound for any value of σ because Γ_s is positive definite and $\tilde{\Psi}$, which represents the uncertainties, has an upper bound (refer to Property 3). Then, the following equation is obtained:

$$\frac{\dot{V}}{2\sqrt{V}} = \Omega(t) - K^*\frac{\sigma^T\Gamma_s\sigma}{\sigma^T\sigma}. \tag{28}$$

According to (18), for $\|\sigma\| > \varepsilon$, K^* continues increasing until the positive scalar $K^*(\sigma^T\Gamma_s\sigma)/(\sigma^T\sigma)$ can compensate for the unknown value of $\Omega(t)$ with an upper bound, i.e.,

$$K^*\frac{\sigma^T\Gamma_s\sigma}{\sigma^T\sigma} > \Omega(t). \tag{29}$$

Thus, there exist a time instant t_* and a positive scalar γ such that

$$K^*\frac{\sigma^T\Gamma_s\sigma}{\sigma^T\sigma} > \Omega(t) + \gamma. \tag{30}$$

In addition, for all $t \ge t_*$, (28) can be rewritten as follows:

$$\dot{V} \le -2\gamma\,\|\sigma\|\,. \tag{31}$$

Therefore, the finite time convergence to a domain $\|\sigma\| \le \varepsilon$ is guaranteed from any initial condition $\|\sigma(0)\| > \varepsilon$. Next, from (31), the following inequality is obtained:

$$\frac{d\sqrt{V}}{dt} = \frac{d}{dt}\,\|\sigma\| \le -\gamma. \tag{32}$$

Then, the maximum convergence time, t_f, can be easily estimated as follows:

$$t_f \le \frac{\|\sigma(t_*) - \varepsilon\|}{\gamma} + t_* \tag{33}$$

where $\varepsilon > 0, t_* > 0$, and $\gamma > 0$. After σ enters the vicinity of the sliding surface (i.e., $\|\sigma\| < \varepsilon$), the switching gain K^* begins to decrease until $K^*(\sigma^T\Gamma_s\sigma)/(\sigma^T\sigma) \le \Omega(t)$, which results in $\dot{V} \ge 0$. However, as soon as σ escapes the boundary (i.e., $\|\sigma\| > \varepsilon$), in accordance with (18), K^* immediately begins to increase again to keep σ in the domain. Thus, K^* continues changing its value near $\Omega(t)$, and σ remains around the boundary layer limit $\|\sigma\| = \varepsilon$. In conclusion, σ initially converges to the bounded domain in finite time and subsequently remains there. Thus, there is a real sliding mode, and Theorem 1 is proven.

Theorem 2: Once the real sliding mode is established within a finite time $t = t_f > 0$, the error dynamics are asymptotically stable on the real sliding surface. Consequently, the state error vectors $e_a, \dot{e}_a, e_u, \dot{e}_u$ converge to zero, which yields $x \to x_d$, $y \to y_d, \delta \to 0$, and $\theta \to 0$.

Proof: To prove Theorem 2, let us first consider the sliding surface of (13) as a linear combination of two independent subsliding surfaces as

$$\sigma = \rho\sigma_1 + \sigma_2 \tag{34}$$

where ρ is an arbitrary constant, and the subsliding surfaces σ_1 and σ_2 are $\dot{e}_a + \lambda_1 e_a$ and $\lambda_2\dot{e}_u + \lambda_3 e_u$, respectively. From Theorem 1, the finite time convergence to a domain $\|\sigma\| \le \varepsilon$ (i.e., the real sliding surface) is guaranteed, which also corresponds to the asymptotic convergence to the equilibrium point $\|\sigma\| = 0$ [50]. Thus, the phase trajectory that moves along the sliding surface σ enters the neighborhood of the coordinate origin, which is constructed by axes σ_1 and σ_2 as $t \to \infty$. Then, the system states that move along the subsliding surfaces σ_1 and σ_2 also move toward, respectively, its coordinate origin constructed by the error state vectors $\dot{e}_a, e_a$ and $\dot{e}_u, e_u$ similar to the movement on the sliding surface σ. This eventually implies $x \to x_d, y \to y_d, \delta \to 0$, and $\theta \to 0$. Theorem 2 is proven.

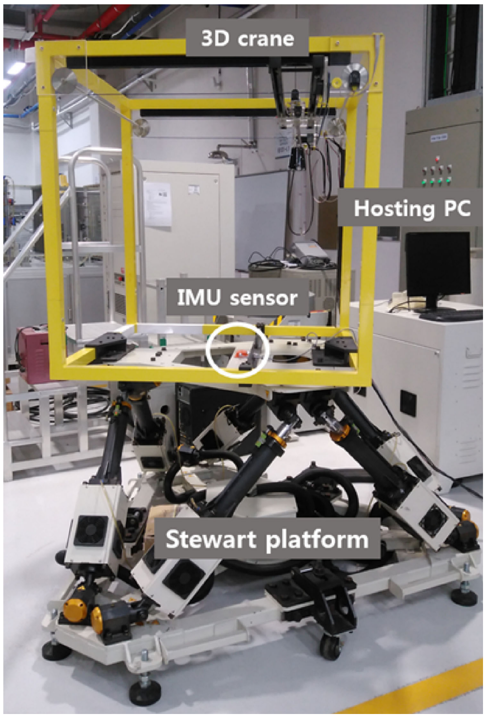

Fig. 3. Experimental setup.

IV. Experiments

A. Experimental Setup

Fig. 3 shows the experimental setup consisting of a 6-DOF Stewart platform and a 3-D crane (INTECO) mounted on the platform. In this experimental testbed, the Stewart platform was utilized to emulate ship motions under the conditions of Sea State 3 (see [1] for more details). The generated ship motions of the platform (i.e., roll motion and pitch motion) were detected online by a high-quality inertial measurement unit (IMU) sensor (MTi sensor, XSENS). Therefore, the 3-D crane placed on the platform can appropriately imitate a ship-mounted container crane. In addition, various actuators and sensors, such as the dc motors and encoders, were installed in the 3-D crane system to control and measure the positions of the trolley and the sway angles of the payload.

The overall control system consist of a hosting PC, which was equipped with an eight-axis multimotion control board (Samsung Electronics Co., Ltd.), an RT-DAC/USB multipurpose digital I/O board, a power interface unit, and the MATLAB/Simulink 2009a real-time Windows target software. Accordingly, control experiments were performed in real time by sending and collecting the control commands and sensor feedback signals with a sampling period (T_s) of 1 ms between the host computer and the sensors/actuators.

B. Experimental Results

Experiments were performed to validate the effectiveness of the proposed control method. Then, the obtained results were compared with other experimental results of the existing works

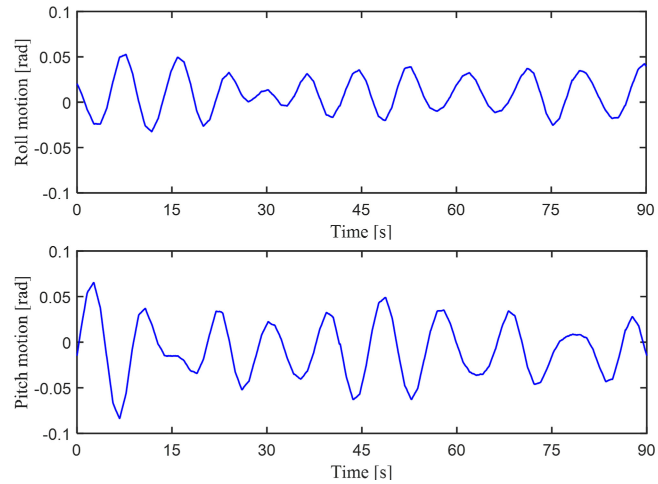

Fig. 4. Generated roll and pitch motions of the ship under Sea State 3 conditions [1].

(i.e., the SMC presented in [2] and the ASMC presented in [49]) to demonstrate the superior performance of the proposed control law. The physical parameters in the experiment were $m_t = 3$ kg, $m_p = 0.73$ kg, $l = 0.32$ m, and $h = 0.9$ m. For simplicity, the slowly varying target positions in the reference coordinate frame were assumed as follows:

$$X_d(t) = 0.12\sin(0.07t) + 0.3,$$
$$Y_d(t) = 0.12\cos(0.07t) + 0.3 \quad (35)$$

which corresponds to a circular motion in the X–Y plane. Then, the desired trajectories $x_d(t)$ and $y_d(t)$ in the crane coordinate frame are computed using (12). The initial conditions were set to

$$x(0) = 0.3 \text{ m}, y(0) = 0 \text{ m},$$
$$\delta(0) \cong 0 \text{ rad}, \theta(0) \cong 0 \text{ rad}. \quad (36)$$

Fig. 4 shows the roll and pitch motions of the ship generated by the Stewart platform assuming the Sea State 3 condition, which were measured with the IMU sensor. Based on repeated experiments under the ideal working condition (i.e., no unknown disturbances except ship motions), the design parameters in (13), (18), and (21) were obtained as follows:

$$K^*(0) = 0.1, \alpha = 3, \beta = 5, \kappa_1 = 4, \kappa_2 = 1.5,$$
$$\varepsilon = 4T_s K, \lambda_{11} = 220, \lambda_{12} = 150,$$
$$\lambda_{21} = 10^{-4}, \lambda_{22} = -10^{-4}, \lambda_{31} = 21, \lambda_{32} = -16. \quad (37)$$

Remark 4: In the ASMC of real sliding mode, a proper choice of ε needs to be made because the overall control performance is directly related to the value. In this paper, parameter ε was determined by following the ε-tuning method, which is known to provide both stability and accuracy for the closed-loop system [51]. Regarding the adaptation parameters κ_1 and κ_2 in (22), they were determined by trial and error upon several experiments: When κ_1 and κ_2 values were too small or too large, an improved

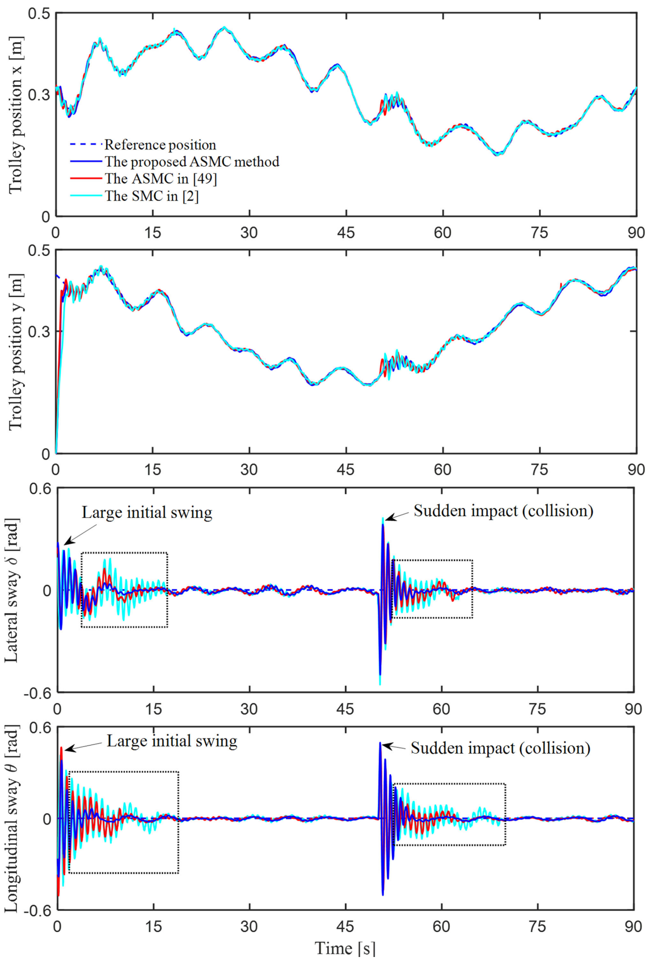

Fig. 5. Comparison of experimental results: trolley movements (x, y) and payload swings (δ, θ).

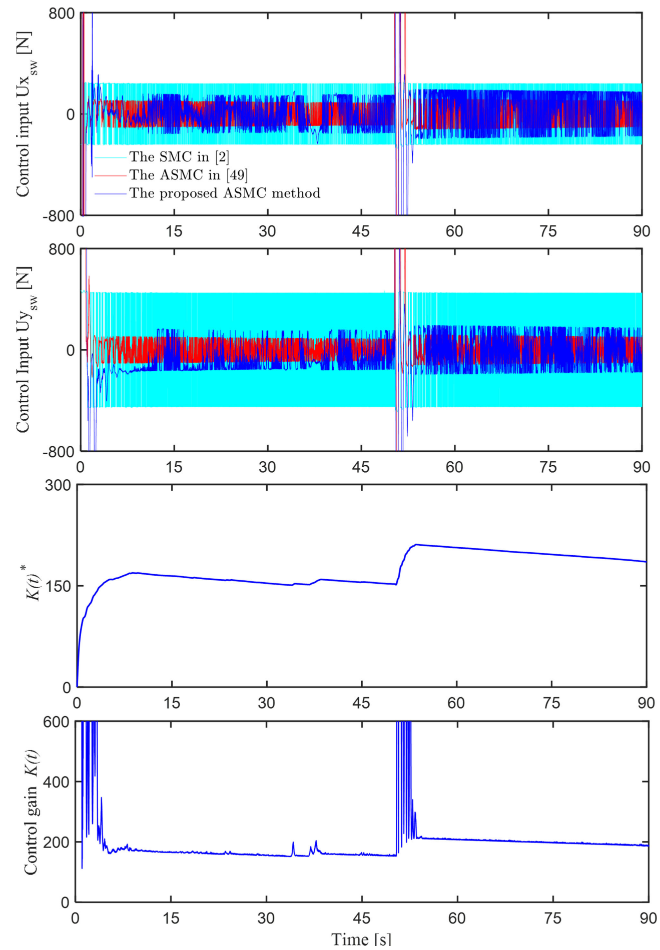

Fig. 6. Comparison of switching control inputs (upper two plots), $K*$ (third), and K (fourth) in (18) of the proposed ASMC.

control performance was not obtained in comparison with the existing methods.

To illustrate the effectiveness of the proposed control law, the obtained results were compared with two existing methods: the SMC method presented in [2] and the ASMC method presented in [49]. Summarizing the SMC in [2] briefly, the law is given as follows:

$$u_{\text{smc}} = u_{\text{eq}} - \Gamma^{-1} K_{\text{smc}} \text{sgn}(\sigma) \tag{38}$$

where the equivalent control law and parameter values of the sliding surface to implement (38) are identical to (20) and (37), respectively, and the gain K_{smc} in (38) was determined by assuming the ideal case (i.e., no disturbance, no parametric uncertainty, only the ship motions exist)

$$K_{\text{smc}} = \begin{bmatrix} 80 & 0 \\ 0 & 150 \end{bmatrix}. \tag{39}$$

The switching term in implementing (38) was replaced by a saturation function to reduce the chattering phenomena of the SMC. Second, in relation to the ASMC method presented in [49], the form of the control law was identical to (17) except the adaptation algorithm (21). For comparison purpose, the design parameter values to implement it were adopted from (37) except κ_1 and κ_2.

To verify the effectiveness of the proposed algorithm, experiments were performed in a harsh operating condition including the following four cases simultaneously.

1) *Condition 1 (wave-induced ship motion):* The ship is oscillating (in Fig. 4, the roll and pitch motions of the ship under Sea State 3 are shown).
2) *Condition 2 (parameter uncertainty):* The parameters that appear in the system model are uncertain (for example, the cargo mass changes from $m_p = 0.73$ kg to 1.4 kg, and the rope length varies from 0.32 to 0.2 m).
3) *Condition 3 (large initial swing):* There is a large initial swing of the payload (in Fig. 5, $\delta(0) \cong 0.25$ rad and $\theta(0) \cong -0.45$rad were set).
4) *Condition 4 (wind-induced sudden impact):* Unknown disturbances, such as wind gusts and collision, can occur (for example, in Fig. 5, at $t = 50$ s, an impact force has been applied to the payload).

Figs. 5–7 compare the obtained experimental results of three methods: the proposed ASMC in this paper, the SMC presented in [2], and the ASMC presented in [49]. The upper two plots in

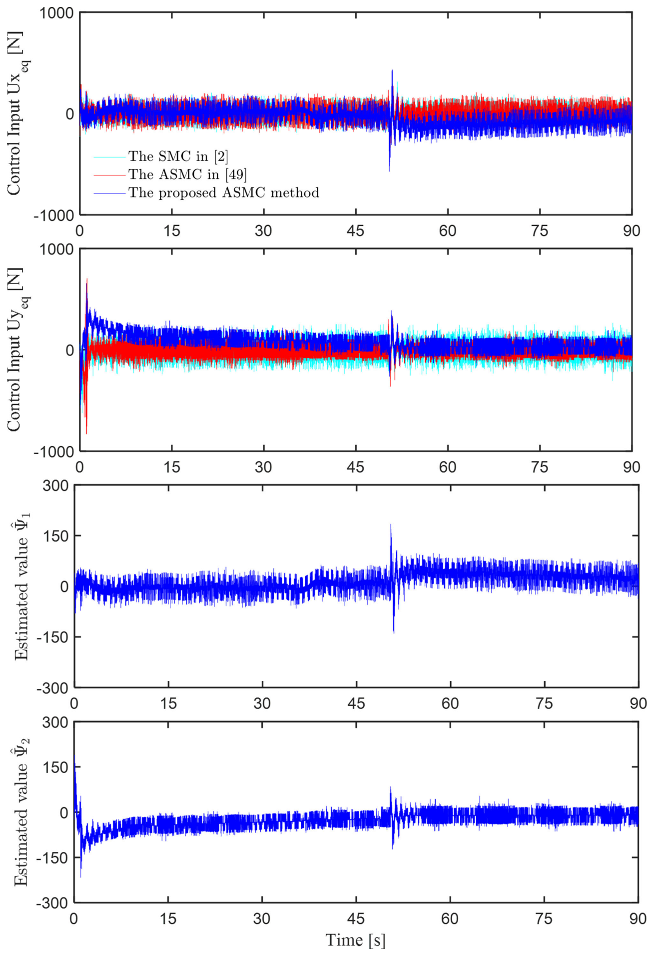

Fig. 7. Comparison of equivalent control inputs (upper two plots) and estimated $\hat{\Psi}$ (bottom two plots) in (22) of the proposed ASMC.

Fig. 5 show that all three methods have a good tracking performance of the reference trajectories in the actuated variables (i.e., the desired trolley displacements $x_d(t)$ and $y_d(t)$) even under the harsh condition. Although the SMC presented in [2] showed a slightly more chattering in the system response when a large initial swing angle was given, the overall control performance was acceptable. However, the bottom two plots in Fig. 5 show that the payload swing angles δ and θ (i.e., the unactuated joint variables) were quite different (in contrast to the actuated variables, x and y) because of the different internal mechanisms in computing the control forces in three methods using the coupling forces between actuated and unactuated variables. In addition, the payload oscillation period (for both a large initial swing angle and a sudden disturbance) lasted longer in the case of the SMC method presented in [2], see the dotted boxes in Fig. 5. The swing reduction time of the proposed ASMC method was achieved within 6 s, whereas that of the SMC method presented in [2] took 16 s. In Fig. 6, the control input of the proposed method reacted faster than the SMC method presented in [2] to compensate the unknown perturbations and achieved the control performance with less chattering in the control input, which is consistent with the theoretical analysis.

Compared with the ASMC of [49], the proposed method also showed better results (blue and red curves in the dotted box in Fig. 5): The sway suppression time was shorter, and the control input had less chattering. Fig. 7 compares the equivalent control inputs of all three cases (see upper two plots). Fig. 7 clearly shows that the equivalent control input of the proposed method actively interacted with the modeling uncertainty and disturbances through the adaptation mechanism of (21), whereas the results of the ASMC in [49] and SMC in [2] had no interaction and showed simple patterns. Thus, the newly proposed adaptation algorithm enables the equivalent control input to effectively eliminate the uncertain system dynamics. Therefore, the overall control performance regarding the chattering and unknown disturbance rejection has been better achieved than the ASMC method presented in [49]. Conclusively, the proposed method is more robust and effective in controlling the offshore container crane suffering from the wave-induced ship motions, parameter uncertainties, and external disturbances with unknown bounds.

Remark 5: For a comprehensive verification of the proposed method, experiments were thoroughly conducted assuming diverse experimental conditions in the combination of ship motions, uncertainties, initial swing, and unknown disturbances. In all of these experiments, the proposed ASMC method with adaptive equivalent control inputs demonstrated a satisfactory performance.

V. Conclusion

This paper investigated a new modeling and ASMC for offshore container cranes in the presence of wave-induced ship motions (i.e., roll and pitch motions), parametric uncertainties, and unknown disturbances. A systematic decoupling method was developed to utilize the internal coupling dynamics (between actuated and unactuated variables) for the sway suppression. Then, a new ASMC method with two adaptation algorithms for switching and equivalent controls was developed based on the composite sliding surfaces constructed by a combination of actuated and unactuated dynamics. The asymptotic stability of the sliding surface was proven by the Lyapunov method without using *a priori* known bounds on the unknown disturbances. The experimental results reveal that our proposed method outperforms the SMC method presented in [2] and the ASMC method presented in [49] under harsh working conditions, including ship roll and pitch motions, weight and length uncertainties, nonzero initial swings, and wind disturbances. In our future studies, the control problem of the offshore container crane subjected to the state constraints and actuator saturation will be investigated.

References

[1] K.-S. Hong and Q. H. Ngo, "Dynamics of the container crane on a mobile harbor," *Ocean Eng.*, vol. 53, pp. 16–24, Oct. 2012.

[2] Q. H. Ngo and K.-S. Hong, "Sliding-mode antisway control of an offshore container crane," *IEEE/ASME Trans. Mechatronics*, vol. 17, no. 2, pp. 201–209, Apr. 2012.

[3] N. Sun, T. Yang, Y. Fang, Y. Wu, and H. Chen, "Transportation control of double-pendulum cranes with a nonlinear quasi-PID scheme: Design and experiments," *IEEE Trans. Syst., Man, Cybern. Syst.*, vol. 49, no. 7, pp. 1408–1418, Jul. 2019.

[4] Z. N. Masoud and A. H. Nayfeh, "Sway reduction on container cranes using delayed feedback controller," *Nonlinear Dyn.*, vol. 34, no. 3-4, pp. 374–358, Dec. 2003.

[5] H. Park, D. Chwa, and K.-S. Hong, "A feedback linearization control of container cranes: Varying rope length," *Int. J. Control Automat. Syst.*, vol. 5, no. 4, pp. 379–387, Aug. 2007.

[6] L. A. Tuan, S.-G. Lee, D. H. Ko, and L. C. Nho, "Combined control with sliding mode and partial feedback linearization for 3D overhead cranes," *Int. J. Robust Nonlinear Control*, vol. 24, no. 18, pp. 3372–3386, Dec. 2014.

[7] N. Sun, T. Yang, H. Chen, Y. Fang, and Y. Qian, "Adaptive anti-swing and positioning control for 4-DOF rotary cranes subject to uncertain/unknown parameters with hardware experiments," *IEEE Trans. Syst., Man, Cybern. Syst.*, vol. 49, no. 7, pp. 1309–1321, Jul. 2019.

[8] N. B. Almutairi and M. Zribi, "Sliding mode control of three-dimensional overhead crane," *J. Vib. Control*, vol. 15, no. 11, pp. 1679–1730, Jul. 2009.

[9] Q. H. Ngo and K.-S. Hong, "Adaptive sliding mode control of container cranes," *IET Control Theory Appl.*, vol. 6, no. 5, pp. 662–668, Mar. 2012.

[10] Q. H. Ngo, N. P. Nguyen, C. N. Nguyen, T. H. Tran, and K.-S. Hong, "Fuzzy sliding mode control of container cranes," *Int. J. Control Automat. Syst.*, vol. 13, no. 2, pp. 419–425, Apr. 2015.

[11] Y. Fang, W. E. Dixon, D. M. Dawson, and E. Zergeroglu, "Nonlinear coupling control laws for an underactuated overhead crane system," *IEEE/ASME Trans. Mechatronics*, vol. 8, no. 3, pp. 418–423, Sep. 2003.

[12] K. Terashima, Y. Shen, and K. Yano, "Modeling and optimal control of a rotary crane using the straight transfer transformation method," *Control Eng. Pract.*, vol. 15, no. 9, pp. 1179–1192, Aug. 2007.

[13] K. L. Sorensen, W. Singhose, and S. Dickerson, "A controller enabling precise positioning and sway reduction in bridge and gantry cranes," *Control Eng. Pract.*, vol. 15, no. 7, pp. 825–837, Jul. 2007.

[14] U. H. Shah and K.-S. Hong, "Open-loop vibration control of an underwater system: Application to refueling machine," *IEEE/ASME Trans. Mechatronics*, vol. 22, no. 4, pp. 1622–1632, Aug. 2017.

[15] R. Olfati-Saber, "Normal forms for underactuated mechanical systems with symmetry," *IEEE Trans. Automat. Control*, vol. 47, no. 2, pp. 305–308, Feb. 2002.

[16] K.-S. Hong, "An open-loop control for underactuated manipulators using oscillatory inputs: Steering capability of an unactuated joint," *IEEE Trans. Control Syst. Technol.*, vol. 10, no. 3, pp. 469–480, May 2002.

[17] X. Yin, Y. Lin, W. Li, H. Liu, and Y. Gu, "Adaptive sliding mode back-stepping pitch angle control of a variable-displacement pump controlled pitch system for wind turbines," *ISA Trans.*, vol. 58, pp. 629–634, Sep. 2015.

[18] X. Yin, Y. Lin, W. Li, Y. Gu, P. Lei, and H. Liu, "Sliding mode voltage control strategy for capturing maximum wind energy based on fuzzy logic control," *Int. J. Elect. Power*, vol. 70, pp. 45–51, Sep. 2015.

[19] N. Sun, Y. Wu, Y. Fang, H. Chen, and B. He, "Nonlinear continuous global stabilization control for underactuated RTAC systems: Design, analysis, and experimentation," *IEEE/ASME Trans. Mechatronics*, vol. 22, no. 2, pp. 1104–1115, Apr. 2017.

[20] C. Mu and H. He, "Dynamic behavior of terminal sliding mode control," *IEEE Trans. Ind. Electron.*, vol. 65, no. 4, pp. 3480–3490, Apr. 2018.

[21] C. Mu, C. Sun, and W. Xu, "Fast sliding mode control on air-breathing hypersonic vehicles with transient response analysis," *Proc. Inst. Mech. Eng. Part I-J. Syst. Control Eng.*, vol. 230, no. 1, pp. 23–34, Jan. 2016.

[22] C. Mu, W. Xu, and C. Sun, "On switching manifold design for terminal sliding mode control," *J. Franklin Inst.-Eng. Appl. Math.*, vol. 353, no. 7, pp. 1553–1572, May 2016.

[23] H. Ma, H. Liang, Q. Zhou, and C. K. Ahn, "Adaptive dynamic surface control design for uncertain nonlinear strict-feedback systems with unknown control direction and disturbances," *IEEE Trans. Syst., Man, Cybern., Syst.*, vol. 49, no. 3, pp. 506–515, Mar. 2019.

[24] H. Ma, H. Liang, H. Ma, and Q. Zhou, "Nussbaum gain adaptive back-stepping control of nonlinear strict-feedback systems with unmodeled dynamics and unknown dead zone," *Int. J. Robust Nonlinear Control*, vol. 28, no. 17, pp. 5326–5343, Sep. 2018.

[25] X. Yin and L. Pan, "Direct adaptive robust tracking control for 6 DOF industrial robot with enhanced accuracy," *ISA Trans*., vol. 72, pp. 178–184, Jan. 2018.

[26] X. Yin and L. Pan, "Enhancing trajectory tracking accuracy for industrial robot with robust adaptive control," *Robot Comput.-Integr. Manuf.*, vol. 51, pp. 97–102, Jun. 2018.

[27] W. Sun, S.-F. Su, Y. Wu, J. Xia, and V.-T. Nguyen, "Adaptive fuzzy control with high-order barrier Lyapunov functions for high-order uncertain nonlinear systems with full-state constraints," *IEEE Trans. Cybern.*, early access, Jan. 15, 2019, doi: 10.1109/TCYB.2018.2890256.

[28] J. Xia, J. Zhang, W. Sun, B. Zhang, and Z. Wang, "Finite-time adaptive fuzzy control for nonlinear systems with full state constraints," *IEEE Trans. Syst., Man, Cybern., Syst.*, vol. 49, no. 7, pp. 1541–1548, Jul. 2019.

[29] W. Sun, S.-F. Su, G. Dong, and W. Bai, "Reduced adaptive fuzzy tracking control for high-order stochastic nonstrict feedback nonlinear system with full-state constraints," *IEEE Trans. Syst., Man, Cybern., Syst.*, early access, Mar. 5, 2019, doi: 10.1109/TSMC.2019.2898204.

[30] P. S. Thakar, P. K. Trivedi, B. Bandyopadhyay, and P. S. Gandhi, "A new nonlinear control for asymptotic stabilization of a class of underactuated systems: An implementation to slosh-container problem," *IEEE/ASME Trans. Mechatronics*, vol. 22, no. 2, pp. 1082–1092, Apr. 2017.

[31] S. Zhang, W. He, and S. S. Ge, "Modeling and control of a nonuniform vibrating string under spatiotemporally varying tension and disturbance," *IEEE/ASME Trans. Mechatronics*, vol. 17, no. 6, pp. 1196–1203, Dec. 2012.

[32] C.-M. Chin, A. H. Nayfeh, and D. T. Mook, "Dynamics and control of ship-mounted cranes," *J. Vib. Control*, vol. 7, no. 6, pp. 891–904, Sep. 2001.

[33] K. Ellermann and E. Kreuzer, "Nonlinear dynamics in the motion of floating cranes," *Multibody Syst. Dyn.*, vol. 9, no. 4, pp. 377–387, May 2003.

[34] Z. N. Masoud, A. H. Nayfeh, and D. T. Mook, "Cargo pendulation reduction of ship-mounted cranes," *Nonlinear Dyn*., vol. 35, no. 3, pp. 299–311, Feb. 2004.

[35] M. P. Spathopoulos and D. Fragopoulos, "Pendulation control of an offshore crane," *Int. J. Control*, vol. 77, no. 7, pp. 654–670, May 2004.

[36] H. Schaub, "Rate-based ship-mounted crane payload pendulation control system," *Control Eng. Pract.*, vol. 16, no. 1, pp. 132–145, Jan. 2008.

[37] A. Maczyński and S. Wojciech, "Stabilization of load's position in offshore cranes," *J. Offshore Mech. Arctic Eng.*, vol. 134, no. 2, May 2012, Art. no. 021101.

[38] Y. Fang, P. Wang, N. Sun, and Y. Zhang, "Dynamics analysis and nonlinear control of an offshore boom crane," *IEEE Trans. Ind. Electron.*, vol. 61, no. 1, pp. 414–427, Jan. 2014.

[39] N. Sun, Y. Fang, H. Chen, Y. Wu, and B. Lu, "Nonlinear antiswing control of offshore cranes with unknown parameters and persistent ship-induced perturbations: Theoretical design and hardware experiments," *IEEE Trans. Ind. Electron.*, vol. 65, no. 3, pp. 2629–2641, Mar. 2018.

[40] N. Sun, Y. Fang, H. Chen, Y. Fu, and B. Lu, "Nonlinear stabilizing control for ship-mounted cranes with ship roll and heave movements: Design, analysis, and experiments," *IEEE Trans. Syst., Man, Cybern., Syst.*, vol. 48, no. 10, pp. 1781–1793, Oct. 2018.

[41] Y.-Z. Qian, Y.-C. Fang, and T. Yang, "An energy-based nonlinear coupling control for offshore ship-mounted cranes," *Int. J. Automot. Comput.*, vol. 15, no. 5, pp. 570–581, Oct. 2018.

[42] Y. Qian, Y. Fang, and B. Lu, "Adaptive repetitive learning control for an offshore boom crane," *Automatica*, vol. 82, pp. 21–28, Aug. 2017.

[43] L. A. Tuan, H. M. Cuong, S.-G. Lee, L. C. Nho, and K. Moon, "Nonlinear feedback control of container crane mounted on elastic foundation with the flexibility of suspended cable," *J. Vib. Control*, vol. 22, no. 13, pp. 3067–3078, Nov. 2014.

[44] L. A. Tuan, S.-G. Lee, L. C. Nho, and H. M. Cuong, "Robust controls for ship-mounted container cranes with viscoelastic foundation and flexible hoisting cable," *J. Syst. Control Eng.*, vol. 229, no. 7, pp. 662–674, Mar. 2015.

[45] R. M. T. R. Ismail, N. D. That, and Q. P. Ha, "Modeling and robust trajectory following for offshore container crane systems," *Automat. Constr.*, vol. 59, pp. 179–187, Nov. 2015.

[46] D. Kim and Y. Park, "Tracking control in *x-y* plane of an offshore container crane," *J. Vib. Control*, vol. 23, no. 3, pp. 469–483, Apr. 2015.

[47] Q. H. Ngo, N. P. Nguyen, C. N. Nguyen, T. H. Tran, and Q. P. Ha, "Fuzzy sliding mode control of an offshore container crane," *Ocean Eng*., vol. 140, pp. 125–134, Aug. 2017.

[48] A. Levant, "Sliding order and sliding accuracy in sliding mode control," *Int. J. Control*, vol. 58, no. 6, pp. 1247–1236, Aug. 1993.

[49] J. Zhu and K. Khayati, "On a new adaptive sliding mode control for MIMO nonlinear systems with uncertainties of unknown bounds," *Int. J. Robust Nonlinear Control*, vol. 27, no. 6, pp. 942–962, Apr. 2017.

[50] F. Plestan, Y. Shtessel, V. Brégeault, and A. Poznyak, "Sliding mode control with gain adaptation—Application to an electropneumatic actuator," *Control Eng. Pract.*, vol. 21, no. 5, pp. 679–688, May 2013.

[51] F. Plestan, Y. Shtessel, V. Brégeault, and A. Poznyak, "New methodologies for adaptive sliding mode control," *Int. J. Control.*, vol. 83, no. 9, pp. 1907–1919, Sep. 2010.

Gyoung-Hahn Kim (S'18) received the B.S. degree in mechanical engineering from Yeungnam University, Gyeongsan, South Korea, in 2013. He is currently working toward the Ph.D. degree in the School of Mechanical Engineering, Pusan National University, Busan, South Korea.

His research interests include mathematical control theory, adaptive sliding-mode control, data-driven control, reinforcement deep learning, and their applications to industrial robotics.

Keum-Shik Hong (S'87–M'91–SM'10–F'19) received the B.S. degree in mechanical design and production engineering from Seoul National University, Seoul, South Korea, in 1979, the M.S. degree in mechanical engineering from Columbia University, New York, NY, USA, in 1987, and the M.S. degree in applied mathematics and the Ph.D. degree in mechanical engineering both from the University of Illinois at Urbana-Champaign, Champaign, IL, USA, in 1991.

From 1982 to 1985, he was with Daewoo Heavy Industries, Incheon, South Korea, where he was engaged in vibration, noise, and emission problems of vehicles and engines. In 1993, he joined the School of Mechanical Engineering, Pusan National University (PNU), where he became a Professor in 2004. His Integrated Dynamics and Control Laboratory was designated as a National Research Laboratory by the Ministry of Education, Science and Technology (MEST) of Korea in 2003. In 2009, under the auspices of the World Class University Program of the MEST of Korea, he established the Department of Cogno-Mechatronics Engineering, PNU. His current research interests include nonlinear systems theory, brain–computer interface, adaptive control, distributed parameter systems, autonomous systems, and innovative control applications in brain engineering.

Dr. Hong serves as the Editor-in-Chief of the *International Journal of Control, Automation and Systems*. He was the Editor-in-Chief of the *Journal of Mechanical Science and Technology* during 2008–2011 and an Associate Editor for *Automatica* during 2000–2006. He was the President of the Institute of Control, Robotics and Systems in 2015 and is the President of the Asian Control Association. He was the recipient of the Presidential Award of Korea in 2007. He is an ICROS Fellow, a Fellow of the Korean Academy of Science and Technology, and a member of the ASME, ICROS, KSME, KSPE, KIEE, KINPR, and the National Academy of Engineering of Korea.